The protein ENH is a cytoplasmic sequestration factor for Id2 in normal and tumor cells from the nervous system

Anna Lasorella and Antonio Iavarone*

Institute for Cancer Genetics, Department of Pathology, Pediatrics, and Neurology, Columbia University Medical Center, New York, NY 10032

Communicated by Mario R. Capecchi, University of Utah, Salt Lake City, UT, January 6, 2006 (received for review November 28, 2005)

Id2 is a natural inhibitor of the basic helix–loop–helix transcription factors and the retinoblastoma tumor suppressor protein. Active Id2 prevents differentiation and promotes cell-cycle progression and tumorigenesis in the nervous system. A key event that regulates Id2 activity during differentiation is translocation from the nucleus to the cytoplasm. Here we show that the actin-associated protein enigma homolog (ENH) is a cytoplasmic retention factor for Id2. ENH contains three LIM domains, which bind to the helix–loop–helix domain of Id proteins *in vitro* and *in vivo*. ENH is up-regulated during neural differentiation, and its ectopic expression in neuroblastoma cells leads to translocation of Id2 from the nucleus to the cytoplasm, with consequent inactivation of transcriptional and cell-cycle-promoting functions of Id2. Conversely, silencing of ENH by RNA interference prevents cytoplasmic relocation of Id2 in neuroblastoma cells differentiated with retinoic acid. Finally, the differentiated neural crest-derived tumor ganglioneuroblastoma coexpresses Id2 and ENH in the cytoplasm of ganglionic cells. These data indicate that ENH contributes to differentiation of the nervous system through cytoplasmic sequestration of Id2. They also suggest that ENH is a restraining factor of the oncogenic activity of Id proteins in neural tumors.

differentiation | enigma homolog | Id proteins | neural cancer

Id2 is one of the four members of the Id protein family, a group of proteins known as inhibitor of differentiation (1, 2). Id2 lies at the center of a molecular network including the retinoblastoma (Rb) tumor suppressor protein and the basic helix–loop–helix (bHLH) transcription factors, the best-known targets for inhibition by Id2 (3, 4). These connections probably operate in a variety of cell types, but our work has characterized them in the nervous system (5–7). In this tissue, overexpression of Id proteins inhibits differentiation whereas ablation of *Id* genes induces premature differentiation of various neural cell types *in vitro* and *in vivo* (8–10). As physiologic regulator of Id2, Rb cooperates with bHLH transcription factors to promote cell-cycle arrest and differentiation in the developing brain. This pathway is subverted in tumor cells. Malignant transformation in the central and peripheral nervous system coincides with frequent elevation of Id2, a process typically implemented by the activation of oncoproteins such as Myc and Ews-Fli1 that up-regulate *Id2* gene transcription, (6, 7, 11, 12). The aberrant accumulation of Id2 contributes to uncontrolled proliferation and neoangiogenesis, two hallmarks of neural cancer (13).

There is general agreement with the notion that differentiation of a variety of cell types requires elimination of Id function. However, the mechanisms by which the signaling pathways initiating differentiation in the nervous system inactivate Id proteins are unknown. Although Id are viewed mainly as nuclear proteins, recent papers reported that relocation of Id proteins to the cytoplasm is an effective way to terminate their activity (10, 14, 15). Interestingly, cytoplasmic sequestration of Id2 has been described in two models of neuroectodermal and hematopoietic differentiation (10, 15). An intriguing model to explain these observations postulates that cytoplasmic factors, activated during differentiation, sequester Id proteins and prevent their import to the nucleus.

Here we identify the actin cytoskeleton-associated PDZ-LIM protein enigma homolog (ENH) as an Id2-associated protein. ENH, whose expression increases during neural differentiation, sequesters Id2 in the cytoplasm and prevents cell-cycle progression and inhibition of bHLH transcription driven by Id2. Furthermore, silencing of ENH by RNA interference abolishes the relocation of Id2 to the cytoplasm in neuroblastoma cells treated with the differentiating agent retinoic acid (RA). We thus identify an antiproliferative and differentiation signaling pathway in the nervous system that converges upon the regulation of ENH. This pathway prevents nuclear retention of Id2 and relieves the inhibitory constraints imposed by Id2 on nuclear transcription factors.

Results

The LIM Domains of ENH Bind to the Helix–Loop–Helix (HLH) Domain of Id Proteins. To identify new interactors of Id2 from the nervous system, we performed yeast two-hybrid screening from a human fetal brain cDNA library using full length Id2 as bait. This screening yielded 47 validated cDNA clones corresponding to four different Id2-associated proteins. Among them, 24 clones code for Id2, 13 clones code for the bHLH transcription factor E2-2, eight clones code for the bHLH transcription factor HEB, and two clones code for the PDZ-LIM protein ENH. All Id2 and bHLH clones retain an intact HLH domain. This finding is consistent with the essential role of the HLH domain for heterodimerization. The presence of endogenous Id2 is explained by the strong homodimerization ability of Id2 and its abundant expression in the fetal brain (16, 17). The identification of two E proteins, E2-2 and HEB, demonstrated that our screening was capable of identifying specific Id2 interactors. The only two clones that did not contain a HLH domain code for ENH, a member of the Enigma family of LIM domain proteins, a class of proteins associated with the actin cytoskeleton (18–21). Proteins of the Enigma family possess an N-terminal PDZ domain and three LIM domains at the C terminus (Fig. 1*A*). All members of the PDZ-LIM Enigma family, including ENH, are cytoplasmic proteins that bind to the actin cytoskeleton through direct interaction between the PDZ domain and α-actinin (19, 20). Sequence analysis of the two ENH clones identified in our two-hybrid assay established that both clones retained a C-terminal fragment of ENH (amino acids 461–596) that includes part of the first and the last two LIM domains but lacked the N-terminal region with the PDZ domain (Fig. 1*A*).

To validate the specificity of the binding between ENH and Id2 and identify the domains that mediate this interaction, we used GST fusion proteins and *in vitro*-translated proteins in pull-down assays. GST-Id2 bound efficiently to *in vitro*-translated, ^{35}S-labeled full-

Conflict of interest statement: No conflicts declared.

Abbreviations: RA, retinoic acid; GNB, ganglioneuroblastoma; siRNA, small interfering RNA; HLH, helix–loop–helix; bHLH, basic HLH; E*n*, embryonic day *n*; VZ, ventricular zone; MZ, mantle zone.

*To whom correspondence should be addressed at: Institute for Cancer Genetics, Columbia University Medical Center, 1150 St. Nicholas Avenue, New York, NY 10032. E-mail: ai2102@columbia.edu.

www.pnas.org/cgi/doi/10.1073/pnas.0600168103

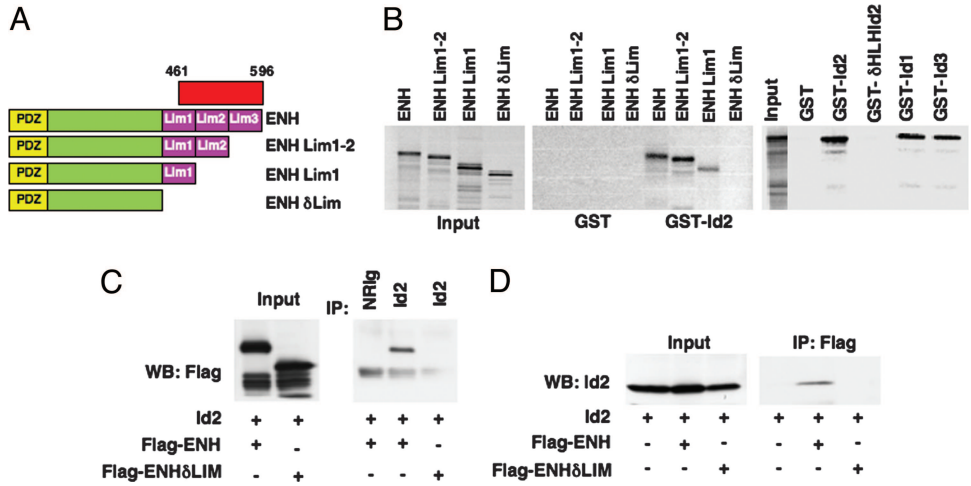

Fig. 1. ENH binds Id2 *in vitro* and *in vivo* through LIM domains. (*A*) Schematic representation of full-length ENH and deletion mutants tested in binding experiments. The C-terminal region of ENH contained in the two clones identified from the two-hybrid screening is shown in red. (*B*) *In vitro*-translated ^{35}S-labeled full-length ENH and LIM domain deletion mutants were mixed with fusion proteins GST, GST-Id2, GST-Id2 lacking the HLH domain (GST-δHLHId2), GST-Id1, and GST-Id3. Bound proteins were analyzed by autoradiography. (*Right*) The lane ''Input'' shows *in vitro*-translated ^{35}S-labeled full-length ENH. Cos-1 cells were transfected with the indicated expression plasmids. Lysates were analyzed directly (Input) or immunoprecipitated with antibodies against Id2 (*C*) or Flag (*D*). Immunoprecipitated proteins were analyzed by Western blot for Flag (*C*) or Id2 (*D*). NRIg, normal rabbit immunoglobulins.

length ENH and to C-terminal ENH deletion constructs that retain two (ENH LIM1–2) or one (ENH LIM1) LIM domains. However, GST-Id2 did not bind to an ENH polypeptide lacking all LIM domains (ENHδLIM) (Fig. 1*B Left* and *Center*). GST-Id2 fusion protein carrying a deletion of the HLH domain (GST-δHLHId2) failed to bind ENH (Fig. 1*B Right*). Given the high homology among the HLH domains of the three Id proteins, we asked whether Id1 and Id3 could also bind ENH in this assay. Indeed, both GST-Id1 and GST-Id3 bound to full-length ENH (Fig. 1*B Right*). To determine whether Id2 binds ENH *in vivo*, we performed coimmunoprecipitation experiments after transfecting Id2 and Flag-tagged ENH in Cos-1. Anti-Id2 antibodies precipitated full-length Flag-ENH but not Flag-ENHδLIM (Fig. 1*C*). Accordingly, Flag-ENH but not Flag-ENHδLIM immunoprecipitates contained Id2 (Fig. 1*D*). Together, these results confirmed that binding of Id2 to ENH occurred through a specific interaction between the LIM domains of ENH and the HLH domain of Id2.

ENH Is Expressed in the Nervous System and Is Induced During Differentiation. The role of ENH has been mostly studied in cardiac and skeletal muscle cells, where ENH has been proposed as a key factor for the integrity of the actin cytoskeleton in differentiated myocytes (19). However, recent reports show that ENH binds to the N-type calcium channel and suggest that a PKC–ENH–calcium channel complex regulates channel activity in neurons (22). Our isolation of ENH from a fetal brain cDNA library suggests that this protein may be implicated in neural development as well. To conduct our study, we raised a polyclonal antibody against a peptide shared by human and mouse ENH. From Western blot experiments, we confirmed that the antibody interacts specifically with exogenously expressed Flag-ENH and endogenous ENH from RA-treated SK-N-SH neuroblastoma cells (Fig. 2*A*). To test whether ENH is expressed during mouse development, we stained sections from embryonic day 15.5 (E15.5) mouse embryo with the anti-ENH antibody. In agreement with published observations, smooth and skeletal muscle cells were strongly stained. At this developmental age, ENH is clearly detectable in neurons from the central nervous system (see the positive ENH staining in spinal cord neurons in Fig. 2*B*) and dorsal root ganglia as well as in chromaffin cells of the adrenal medulla, thus suggesting that expression of ENH is more widespread than it has been previously reported (Fig. 2*B*; see also Fig. 6*C* and data not shown for dorsal root ganglia).

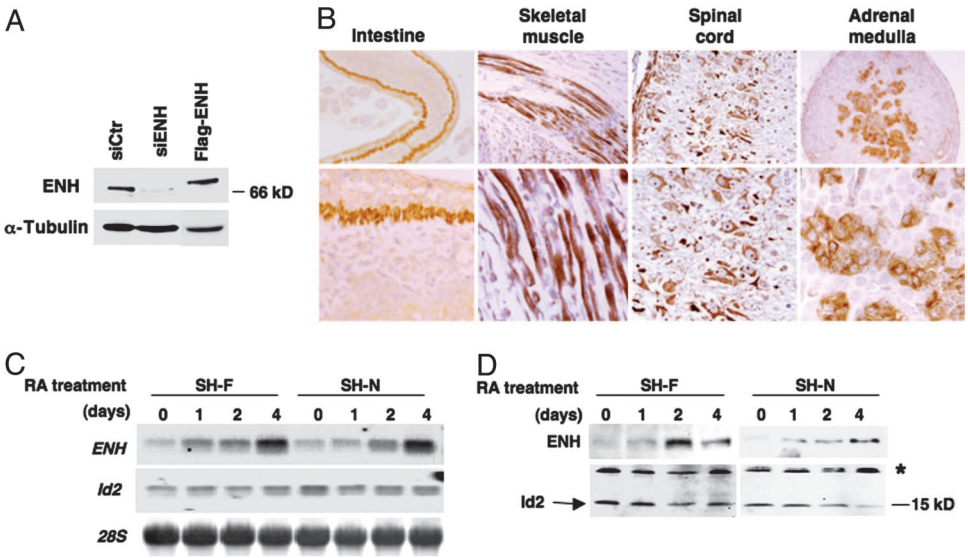

Fig. 2. ENH is expressed in muscle and neural tissues and is up-regulated in neuroblastoma cells treated with RA. (*A*) Western blot analysis shows specificity of the ENH antibody for endogenous ENH in RA-treated SK-N-SH cells and ectopically expressed Flag-ENH. The ENH band is lost after treatment of the cells with siRNA oligonucleotides to ENH (*siENH*). *SiCtr* is a smart-pool siRNA mixture to luciferase (Dharmacon). (*B*) ENH immunohistochemistry from E15.5 mouse embryo shows expression in neural and muscle tissues. [Magnification: ×20 (*Upper*) and ×100 (*Lower*).] (*C*) Northern Blot analysis of *ENH* and *Id2* in SH-F and SH-N cells treated with RA for the indicated times. *28S* rRNA is shown as a loading control. (*D*) Lysates from parallel cultures were analyzed by Western blot by using ENH and Id2 antibodies. The asterisk indicates a nonspecific band.

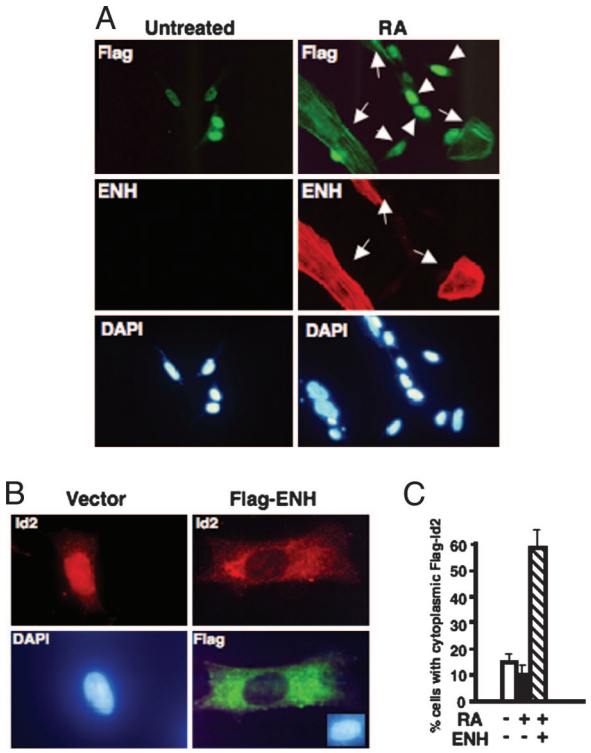

Fig. 3. ENH relocates Id2 to the cytoplasm. (*A*) SK-N-SH cells expressing Flag-Id2 were treated with RA or vehicle control for 48 h. Cells were double-immunostained for Flag (green) and ENH (red). Nuclei were counterstained with DAPI (blue). Arrows indicate cells showing coexpression of cytoplasmic Flag-Id2 and ENH. Arrowheads indicate cells with nuclear Flag-Id2 that lack ENH. (*B*) SK-N-SH cells were transiently transfected with Flag-ENH and immunostained for endogenous Id2 (red) and Flag (green). Nuclei were counterstained with DAPI. (*C*) Quantitative analysis of SK-N-SH cells displaying cytoplasmic Flag-Id2 from the experiment shown in *A* (at least 300 cells were scored for each sample).

Human neuroblastoma cells are frequently used as *in vitro* models to recapitulate differentiation of the nervous system (23, 24). To ask whether ENH expression is regulated during differentiation of the nervous system we used clonal derivatives of the human neuroblastoma cell line SK-N-SH, the SK-N-SH-N (SH-N) and SK-N-SH-F (SH-F) cells. These cells, which lack *N-myc* gene amplification, have been used to characterize the cell-cycle exit associated with differentiation of neural cells (25). When treated with a low concentration of RA (0.1 μM) SH-N cells undergo differentiation along the neuronal lineage, whereas SH-F cells acquire an epithelioid morphology and rapidly enter into a senescent-like state. Both cell types arrest in the G_1 phase of the cell cycle within 48 h of treatment with RA (25). Remarkably, RA induced progressive elevation of ENH mRNA and protein in SH-N and SH-F cells, suggesting that ENH may play a role in multiple differentiation pathways in the nervous system (Fig. 2 *B* and *C*). Although higher concentrations of RA led to marked inhibition of *N-myc* and *Id2* gene expression in *N-myc*-amplified neuroblastoma cells (13), we noted that RA at the concentration of 0.1 μM caused little change of Id2 expression in the SK-N-SH derivatives. However, a late decrease of Id2 protein was evident in RA-treated SH-N cells (Fig. 2*D*).

ENH Is Essential for Cytoplasmic Relocation of Id2 in Neuroblastoma Cells Treated with RA. We sought to ask whether elevation of ENH in RA-treated neuroblastoma cells leads to sequestration of Id2 in the cytoplasm by two independent experimental approaches. First, we examined the subcellular localization of Flag-Id2 after treatment with RA of SK-N-SH using double immunofluorescence staining of endogenous ENH and Flag. Flag-Id2 was predominantly nuclear in untreated cells (Fig. 3*A Top Left*). In agreement with results shown in Fig. 2, logarithmically growing neuroblastoma cells showed minimal ENH staining (Fig. 3*A Middle Left*). After treatment with RA, Flag-Id2 relocated to the cytoplasm in cells that had acquired high ENH expression (Fig. 3*A Top Right*, arrows; see also *Middle* for expression of ENH in the same cells) but remained nuclear in ENH-negative cells (Fig. 3*A Top Right*, arrowheads). Quantitative analysis of the subcellular localization of Id2 and ENH from three independent experiments demonstrated that, after treatment with RA, Flag-Id2 relocated to the cytoplasm in ≈60% of the ENH-positive cells compared with 10% of the ENH-negative cells and 15% of untreated cells (Fig. 3*C*). Next we introduced ectopic Flag-ENH in SK-N-SH and examined the subcellular localization of endogenous Id2. Ectopic ENH localized to the cytoplasm with a pattern compatible with actin stress fibers (Fig. 3*B Lower Right*). As expected, Id2 was mainly nuclear in cells transfected with empty vector (Fig. 3*B Left*). However, expression of ENH caused translocation of Id2 to the cytoplasm (Fig. 3*B Upper Right*).

To establish the functional significance of endogenous ENH for the cytoplasmic relocation of Id2 induced by RA, we took advantage of a loss-of-function approach using small interfering RNA (siRNA) oligonucleotides directed to ENH. Transfection of RA-treated SK-N-SH with siRNA targeting ENH resulted in efficient depletion of ENH from these cells (Fig. 2*A*). Flag-Id2 translocated to the cytoplasm of RA-treated SK-N-SH in the presence of scrambled siRNA oligonucleotides, but the siRNA-mediated silencing of ENH prevented entirely the RA-induced relocation of Flag-Id2 to the cytoplasm (Fig. 4*A*; see also Fig. 4*B* for the quantitative analysis of subcellular localization of Flag-

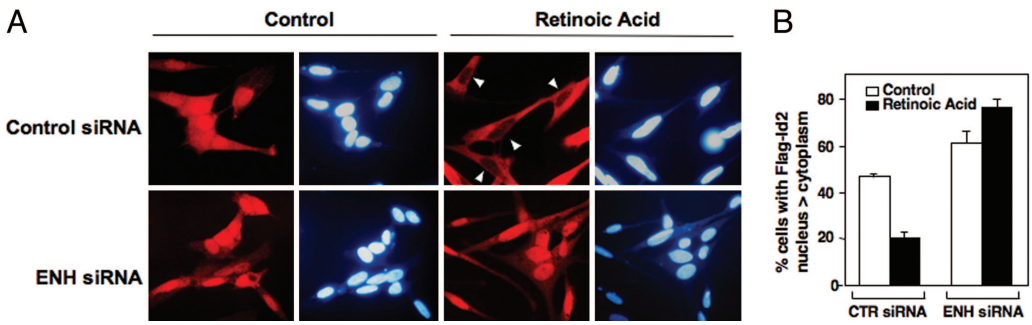

Fig. 4. ENH knockdown prevents translocation of Id2 to the cytoplasm in neuroblastoma cells treated with RA. (*A*) Control (scrambled) or ENH-specific siRNA oligonucleotides were introduced in SK-N-SH expressing Flag-Id2 before treatment with RA or vehicle control for 72 h. Cells were immunostained for Flag-Id2 (red) and counterstained with DAPI. Arrowheads indicate cells displaying full relocation of Flag-Id2 to the cytoplasm after treatment with RA. (*B*) Quantitative analysis of cells displaying predominant nuclear Flag-Id2 (at least 500 cells were scored for each sample).

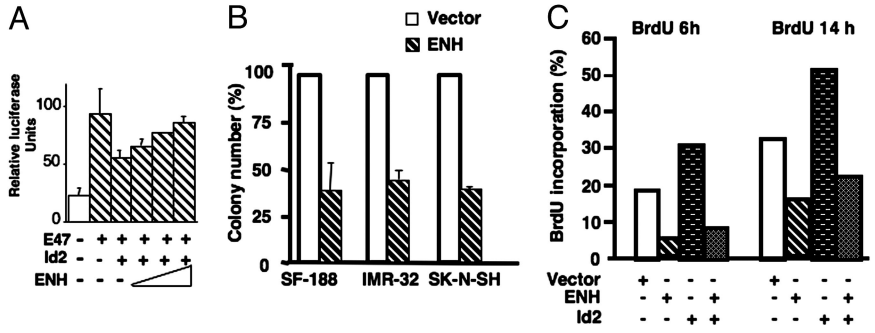

Fig. 5. ENH inhibits proliferation and Id2-mediated functions. (*A*) IMR32 neuroblastoma cells were transfected with a multimerized E-box-luciferase plasmid plus expression plasmids for the indicated proteins. Cotransfection of increasing concentrations of ENH (0.375, 0.5, and 0.625 μg) relieved transcriptional inhibition by Id2. Results of luciferase activity are expressed as means of quadruplicate assays normalized for transfection efficiency by using β-galactosidase (error bars indicate standard deviations). (*B*) SK-N-SH, IMR-32 (neuroblastoma), and SF188 (glioma) were transfected with ENH or the empty vector, and colonies were scored after selection in G418. The total number of colonies recovered from the empty vector control transfection of each cell line were as follows: SF188, 168; IMR32, 223; SK-N-SH, 121. (*C*) SK-N-SH cells were transfected with the indicated plasmid combinations. A plasmid encoding GFP was included to identify transfected cells. Cultures were labeled with BrdU for 6 h and 14 h and immunostained for BrdU by using a Cy3-conjugated secondary antibody. Cells were assessed for GFP and BrdU, and the percentage of transfected cells positive for BrdU was scored.

Id2). Together, these results indicate that activation of ENH expression by RA is essential for cytoplasmic sequestration of Id2 in neuroblastoma.

ENH Counters Id2 Activity and Is an Inhibitor of Proliferation and Cell-Cycle Progression. To test the hypothesis that ENH restrains the inhibitory effects of Id2 on bHLH-mediated transcription by acting as a cytoplasmic retention factor for Id2, we performed luciferase reporter assays with five multimerized E-boxes driving expression of luciferase (E-box-luc). We transfected the E-box-luc plasmid in the presence of mammalian expression vectors for the ubiquitously expressed bHLH protein E47, Id2, and increasing amounts of ENH. Id2 inhibition of E47-mediated transcription was relieved by coexpression of ENH in a dose-dependent manner (Fig. 5*A*). A well known function of Id2 is the ability to enhance cell proliferation by promoting the transition from G_1 to S phase of the cell cycle (6, 7). Therefore, we asked whether ENH inhibited cell proliferation and opposed Id2-mediated entry into S phase. Expression of ENH in three human neuroectodermal cell lines (the glioma cell line SF188 and the neuroblastoma cell lines IMR-32 and SK-N-SH) markedly inhibited colony formation, suggesting that ENH has antiproliferative effects (Fig. 5*B*). Next we transfected SK-N-SH with ENH and Id2 in the presence of a GFP expression plasmid and measured the rate of DNA synthesis by incorporation of BrdU of the successfully transfected, GFP-positive cells. Ectopic ENH strongly inhibited S phase entry and abrogated the Id2-mediated stimulation of DNA synthesis (Fig. 5*C*). These results suggest that, through its ability to sequester Id2 in the cytoplasm, ENH can efficiently suppress the functions of Id2 requiring nuclear localization, including the stimulation of cell-cycle progression.

The ENH-Id2 Pathway in Development and Cancer from the Nervous System. Taken together, the above findings indicate that, even when ectopically expressed, Id2 may be efficiently inactivated through cytoplasmic relocation implemented by differentiation signals that converge upon up-regulation of ENH. To test this hypothesis in a genetic mouse model *in vivo*, we generated transgenic mice expressing *Flag-Id2* from the neural-specific promoter *Nestin*. We established six independent *Nestin-Flag-Id2* mouse transgenic lines. We confirmed that Flag-Id2 is expressed in the telencephalon of hemizygous embryos by Western blot (Fig. 6*A*) and immunohistochemistry (Fig. 6*C Upper*). The older transgenic mice of this colony are >1 year old. We did not observe any abnormality in growth and differentiation of the nervous system during embryogenesis or postnatal life of *Nestin-Flag-Id2* transgenics. Thus, we took advantage of this transgenic system to ask whether normal differentiation in the nervous system requires ENH-mediated relocation of Id2 to the cytoplasm. First, we used coimmunoprecipitation experiments to show that Flag-Id2 interacted specifically with endogenous ENH in *Nestin-Flag-Id2* transgenic brains (Fig. 6*B*). Next, we performed immunohistochemistry for Flag and ENH on adjacent sections of the telencephalon at E15.5. At this developmental age, active proliferation of neural precursors is present in the periventricular, germinal layer [ventricular zone (VZ)], whereas differentiated neurons migrate radially and enter the mantle zone (MZ), which contains postmitotic cells. Flag-Id2 was predominantly nuclear in the neural precursors of the VZ but relocated to the cytoplasm in the differentiating neurons migrating toward the MZ (Fig. 6*C Upper*). Interestingly, ENH was barely detectable in the proliferating and undifferentiated precursors of the VZ but was coexpressed with Id2 in the cytoplasm of differentiated neurons (Fig. 6*C Lower*). These findings suggest that ENH is a component of the physiologic neural differentiation machinery that promotes cytoplasm relocation of Id2 in the developing brain.

Our earlier work established that Id2 displays predominant nuclear expression in aggressive neuroblastoma, an undifferenti-

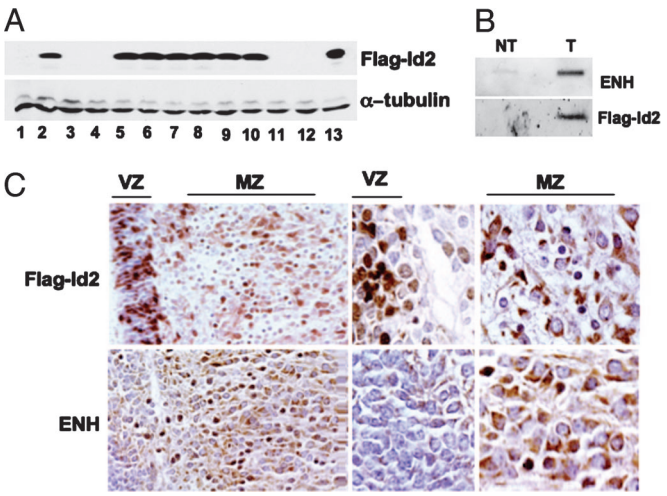

Fig. 6. Cytoplasmic translocation of Flag-Id2 in *Nestin-Flag-Id2* transgenic mouse brain is associated with expression of ENH in differentiating cells. (*A*) Western blot of E15.5 brains from two transgenic lines (lanes 1–5, line 1; lanes 6–12, line 2) for Flag-Id2 shows expression of Flag-Id2 in hemizygous transgenic embryos (lanes 2 and 5–10) but not wild-type embryos (lanes 1, 3, 4, 11, and 12). Lane 13 is the positive control of SK-N-SH expressing Flag-Id2. α-Tubulin is shown as a control for loading. (*B*) Lysates from whole brain of *Nestin-Flag-Id2* transgenic (T) and control (NT) pups were immunoprecipitated with anti-Flag M2 antibody and analyzed for ENH and Flag-Id2 by Western blot. (*C*) Adjacent sections from the brain of E15.5 *Nestin-Flag-Id2* embryos were immunostained for Flag and ENH. [Magnification: $\times$20 (*Left*) and $\times$100 (*Center* and *Right*; magnification of the VZ and MZ).] Nuclear Flag-Id2 is detected in the VZ, which expresses barely detectable ENH. Strong expression of ENH in the MZ is associated with cytoplasmic relocation of Flag-Id2.

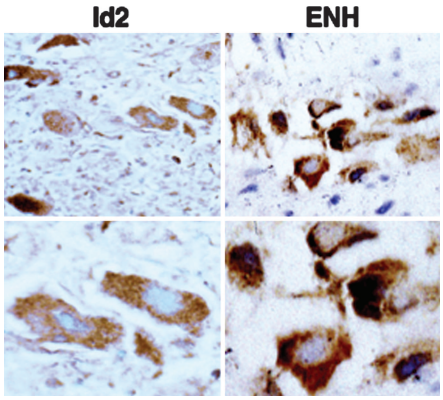

Fig. 7. Id2 and ENH localize to the cytoplasm of differentiated tumor cells in GNB. Id2 and ENH antibodies were used to immunostain primary tumors (brown precipitates). [Magnification: ×20 (*Upper*) and ×100 (*Lower*).]

ated form of pediatric tumor derived from the neural crest (6). A more differentiated form of these tumors, the ganglioneuroblastoma (GNB), is characterized by the presence of a differentiated cellular component interspersed within a predominant, undifferentiated population of cells (26). To determine whether ENH may regulate the subcellular compartmentalization of Id2 in primary neural tumors, we compared the expression of ENH and Id2 in four GNBs by immunostaining tumor sections with antibodies against Id2 and ENH. Most of the tumor cells stained negative for both ENH and Id2. However, we detected cytoplasmic accumulation of Id2 in the mature ganglionic cells of these tumors. Interestingly, the cytoplasm of the same cells was markedly positive for ENH. Representative images are shown in Fig. 7.

The tumor expression data support our findings in cell culture and embryonic mouse brain and further strengthen the hypothesis that differentiation of neural cells requires ENH to sequester Id2 in the cytoplasm.

Discussion

Regulation of transcription factors by subcellular compartmentalization has been demonstrated in a number of cases (27). A common mechanism elicited in this process is sequestration of the factor into inactive compartments, usually through direct or indirect association with the cytoskeleton (28–33). The cellular localization of Id2 was recently proposed to be critical for the regulation of Id2 function (10, 14, 15). Id2 activity is primarily executed in the nucleus, where the Id2 protein antagonizes the function of DNA-binding proteins and pocket proteins of the Rb family (4, 34). Although other biological conditions may regulate subcellular compartmentalization of Id2, the process of differentiation, associated with the state of proliferative quiescence, requires nuclear exclusion of Id2 (10, 14, 15). Here we have found that the cytoskeleton-associated protein ENH binds and sequesters Id2 in the cytoplasm, thus preventing its nuclear actions.

ENH belongs to a growing family of adaptor proteins that are anchored to the actin cytoskeleton through the PDZ domain and direct LIM-associated partners to actin filaments (18). The LIM domains of ENH are cysteine-rich double zinc finger motifs, which are known to mediate protein–protein interactions (35). They contact the HLH domain of Id2. Interestingly, there are previous examples of interactions between the HLH and the LIM domains. These include binding between the bHLH protein TAL1 and the LIM transcription factor LMO2, as well as the interaction of MyoD, MRF4, and myogenin with MLP, another LIM protein (36, 37). These associations occur in the nucleus and determine the composition of particular transcription complexes. Our findings suggest that the LIM–HLH interaction is also used by ENH to inhibit nuclear shuttling of Id2 and drive differentiation. Knockdown of ENH had marked consequences on the cytoplasmic translocation of Id2 promoted by treatment of neuroblastoma cells with RA, a powerful inhibitor of cell proliferation and inducer of multiple pathways of differentiation. By anchoring itself to the actin cytoskeleton through the N-terminal PDZ domain, ENH tethers Id2 to the cytoskeleton. This mechanism recapitulates that ascribed to other cytoskeleton-associated proteins for their ability to sequester transcription factors in the cytoplasm (28–33). Although we have been focused primarily on the functional interaction between ENH and Id2 in neural cells, the ability of ENH to bind other Id proteins combined with its participation in differentiation of other tissue types (e.g., muscle) suggests that ENH may be a general inducer of differentiation through binding and cytoplasmic sequestration of Id proteins. Recently, additional isoforms of ENH (ENH2, ENH3, and ENH4) have been identified in human and mouse muscle tissues (19, 38). These isoforms lack the three LIM domains and resemble the ENHδLIM mutant tested by us in Fig. 1 *A* and *B*. Based on our results, we conclude that the alternative ENH isoforms are unable to bind Id2, a property that might contribute to a potential dominant-negative activity toward full-length ENH (ENH1) *in vivo* (19, 38).

Id proteins are aberrantly accumulated in various forms of human cancer, where they drive multiple hallmarks of neoplasia (34). The most common mechanism selected by tumor cells to activate Id function is to elevate the expression of *Id* genes through oncogenic activation of the upstream transcriptional enhancers. Now we suggest that tumor cells may also target another level of regulation of the Id biology. Our findings in GNB implicate that, by limiting the access of Id2 to the nuclear targets, expression of ENH may be a crucial safeguard against full-blown anaplasia in more differentiated tumors. As we have shown for ENH, other members of the PDZ-LIM domain family of proteins are more abundantly expressed in nontransformed cells and suppress growth of tumor cells (39–41). It is likely that this is a general attribute of this family of proteins. It will be interesting to test whether the most aggressive forms of human neoplasm select genetic and/or epigenetic alterations of the genes coding for PDZ-LIM proteins.

Materials and Methods

Yeast Two-Hybrid Screening. The Proquest system (Life Technologies) was used for yeast two-hybrid screening. The entire coding sequence of human Id2 was subcloned into the bait plasmid pDBLeu. A human fetal brain cDNA library in pPC86 (Life Technologies) was transformed into MaV203 yeast cells and screened for interactors with the bait plasmid according to the manufacturer's protocol.

Cell Culture, Colony-Forming Assay, and Transfection. Neuroblastoma cell lines SK-N-SH, IMR-32, and LAN-1, the glioma cell line SF188, and COS-1 cells were maintained in 10% FBS (Sigma) in DMEM (Cambrex). For colony-forming assay cells were transfected with pcDNA3-ENH or vector control. Cells were selected in G418 for 14 days, and colonies were scored in triplicate cultures. Cells were transfected by using Lipofectamine 2000 according to the manufacturer's instructions.

Northern Blot. RNA was isolated by the TRIzol (Invitrogen) method. Twenty micrograms of total RNA was electrophoresed on an agarose-formaldehyde gel and transferred to nylon membrane (Nytran SPC; Schleicher & Schuell). cDNA of human ENH was used as a probe.

GST Pull-Down Assay, Western Blot, and Coimmunoprecipitation. GST fusion proteins were purified from BL21 Star (Invitrogen). GST pull-down assay was performed as described (42, 43). For Western blot analysis cellular pellets were lysed in ice-cold RIPA buffer (50 mM Tris, pH 7.5/150 mM NaCl/1% Nonidet P-40/0.5% sodium

deoxycholate/0.1% SDS) containing Complete Mini protease inhibitor pellet (Roche) and 1 mM PMSF. Lysates were electrophoresed on SDS/PAGE gels and transferred to nitrocellulose membrane (Amersham Pharmacia Biotech). Membranes were stained with antibodies against ENH, Id2 (Santa Cruz Biotechnology), and α-tubulin (Sigma), and blots were developed by using ECL Western Blotting Detection System (Amersham Pharmacia Biotech). The anti-ENH antibody is a rabbit polyclonal that was produced in collaboration with Zymed against a peptide that is fully conserved in the mouse sequence (KQQNGPPRKHI). Coimmunoprecipitation of Id2 and ENH from cells transfected with pcDNA.3-Id2 and p3XFlag-ENH was performed as described (44).

Luciferase Assay. The luciferase reporter construct 5xE-box-luciferase (43) was cotransfected with pcDNA.3-E47 and pcDNA.3 vector or pcDNA.3-Id2 and pcDNA.3-ENH into SK-N-SH cells. pCMV-β-gal was cotransfected for normalization. Twenty-four hours later luciferase and β-galactosidase activities were measured as described (7).

BrdU Incorporation Study. SK-N-SH cells were plated in Lab-Tek Chamber Slides (Nalge Nunc). Cells were transfected with plasmids expressing the empty vector, Id2, ENH, or both and an EGFP expression vector to identify transfected cells. After 24 h, cells were labeled with 10 μM BrdU for 6 h and 14 h, fixed, and stained with anti-BrdU antibody (Roche) for 1 h at room temperature. Secondary antibody was donkey anti-mouse, Cy3-conjugated (Jackson ImmunoResearch). Nuclei were counterstained with DAPI. Cells were examined on an Olympus epifluorescence microscope. BrdU-positive cells were scored by counting at least 500 GFP-positive cells in three independent experiments.

Quantitative Analysis of Subcellular Localization of Id2 and siRNA Experiments. SK-N-SH-Flag-Id2 cells untreated or treated with RA for 48 h were fixed in 4% paraformaldehyde. Flag-Id2 and endogenous ENH were immunostained by using Flag-M2 (Sigma) and ENH antibodies, respectively. SK-N-SH cells were transfected with vector or p3XFlag-ENH and immunostained by using Flag-M2 and Id2 (Zymed) antibodies. For silencing of ENH, ENH siRNA (siGenome Smartpool reagent M-006930-00) and control, nontargeting (siGenome Smartpool reagent D-001206-13) siRNA mixtures were purchased from Dharmacon. SK-N-SH cells stably expressing Flag-Id2 were treated with vehicle control or RA for 48 h and transfected with 60 nM siRNAs by using Lipofectamine 2000 (Invitrogen). Thirty-six hours after transfection cells were fixed in 4% paraformaldehyde and immunostained by using Flag-M2 antibodies. Parallel cultures were analyzed by Western blot. Secondary antibodies were FITC- or Cy3-conjugated anti-rabbit and Cy3-conjugated anti-mouse (Jackson ImmunoResearch). Nuclei were counterstained with DAPI. Slides were mounted in 90% glycerol in PBS and analyzed on an Olympus epifluorescence microscope. The percentage of cells displaying Id2 staining in the nucleus was scored by counting at least 500 cells from triplicate samples.

Transgene Construction, Generation, and Screening of Mice. To direct transgenic expression of Id2, Flag-tagged *Id2* cDNA was driven by the enhancer element contained in the second intron of the *Nestin* gene coupled with the *thymidine kinase* minimal promoter (45). The second intron of the *Nestin* gene directs expression in central nervous system progenitor cells. The first intron from the rat *insulin II* gene was included to enhance expression levels (46). The transgene fragment was microinjected at a concentration of 6 ng/μl into fertilized mouse eggs. Transgenic mice were identified by PCR analysis of DNA samples prepared from tail biopsies.

Immunohistochemistry. GNB sections were from anonymous tumors stored in the Columbia University tumor bank. Sections from E15.5 mouse brain or primary tumors were deparaffinized in xylenes and rehydrated in a graded series of ethyl alcohol. Primary antibodies were Flag-M2 (Sigma), Id2, and ENH (Zymed). Avidin–biotin–peroxidase complex technique was used for primary antibody detection (Vectastain kit; Vector Laboratories). Staining was developed by using diaminobenzidine (brown precipitate). Sections were counterstained with hematoxylin. Rabbit or mouse IgG (Vector Laboratories) and tissue from *Id2*$-/-$ mice were routinely used as controls for specificity of the staining.

We thank Takuma Uo for help with GST pull-down experiments and Emerson King for establishment of the *Nestin-Flag-Id2* transgenic mouse colony. We thank Anjen Chenn (Northwestern University, Chicago) for the *Nestin* promoter construct and Harshwardhan Thaker (Columbia University Medical Center) for GNB tumor sections. This work was supported by National Institutes of Health/National Cancer Institute Grants R01-CA101644 (to A.L.) and R01-CA85628 (to A.I.) and a grant from the Charlotte Geyer Foundation (to A.I.).

1. Norton, J. D., Deed, R. W., Craggs, G. & Sablitzky, F. (1998) *Trends Cell Biol.* **8,** 58–65.
2. Norton, J. D. (2000) *J. Cell Sci.* **113,** 3897–3905.
3. Ruzinova, M. B. & Benezra, R. (2003) *Trends Cell Biol.* **13,** 410–418.
4. Lasorella, A., Uo, T. & Iavarone, A. (2001) *Oncogene* **20,** 8326–8333.
5. Iavarone, A. & Lasorella, A. (2004) *Cancer Lett.* **204,** 189–196.
6. Lasorella, A., Boldrini, R., Dominici, C., Donfrancesco, A., Yokota, Y., Inserra, A. & Iavarone, A. (2002) *Cancer Res.* **62,** 301–306.
7. Lasorella, A., Noseda, M., Beyna, M., Yokota, Y. & Iavarone, A. (2000) *Nature* **407,** 592–598.
8. Lyden, D., Young, A. Z., Zagzag, D., Yan, W., Gerald, W., O'Reilly, R., Bader, B. L., Hynes, R. O., Zhuang, Y., Manova, K. & Benezra, R. (1999) *Nature* **401,** 670–677.
9. Toma, J. G., El-Bizri, H., Barnabe-Heider, F., Aloyz, R. & Miller, F. D. (2000) *J. Neurosci.* **20,** 7648–7656.
10. Wang, S., Sdrulla, A., Johnson, J. E., Yokota, Y. & Barres, B. A. (2001) *Neuron* **29,** 603–614.
11. Fukuma, M., Okita, H., Hata, J. & Umezawa, A. (2003) *Oncogene* **22,** 1–9.
12. Nishimori, H., Sasaki, Y., Yoshida, K., Irifune, H., Zembutsu, H., Tanaka, T., Aoyama, T., Hosaka, T., Kawaguchi, S., Wada, T., *et al.* (2002) *Oncogene* **21,** 8302–8309.
13. Lasorella, A., Rothschild, G., Yokota, Y., Russell, R. G. & Iavarone, A. (2005) *Mol. Cell. Biol.* **25,** 3563–3574.
14. Kurooka, H. & Yokota, Y. (2005) *J. Biol. Chem.* **280,** 4313–4320.
15. Tu, X., Baffa, R., Luke, S., Prisco, M. & Baserga, R. (2003) *Exp. Cell Res.* **288,** 119–130.
16. Liu, J., Shi, W. & Warburton, D. (2000) *Biochem. Biophys. Res. Commun.* **273,** 1042–1047.
17. Neuman, T., Keen, A., Zuber, M. X., Kristjansson, G. I., Gruss, P. & Nornes, H. O. (1993) *Dev. Biol.* **160,** 186–195.
18. Khurana, T., Khurana, B. & Noegel, A. A. (2002) *Protoplasma* **219,** 1–12.
19. Nakagawa, N., Hoshijima, M., Oyasu, M., Saito, N., Tanizawa, K. & Kuroda, S. (2000) *Biochem. Biophys. Res. Commun.* **272,** 505–512.
20. Vallenius, T., Luukko, K. & Makela, T. P. (2000) *J. Biol. Chem.* **275,** 11100–11105.
21. Ueki, N., Seki, N., Yano, K., Masuho, Y., Saito, T. & Muramatsu, M. (1999) *J. Hum. Genet.* **44,** 256–260.
22. Maeno-Hikichi, Y., Chang, S., Matsumura, K., Lai, M., Lin, H., Nakagawa, N., Kuroda, S. & Zhang, J. F. (2003) *Nat. Neurosci.* **6,** 468–475.
23. Abemayor, E. & Sidell, N. (1989) *Environ. Health Perspect.* **80,** 3–15.
24. Sidell, N., Sarafian, T., Kelly, M., Tsuchida, T. & Haussler, M., IV (1986) *Exp. Cell Biol.* **54,** 287–300.
25. Wainwright, L. J., Lasorella, A. & Iavarone, A. (2001) *Proc. Natl. Acad. Sci. USA* **98,** 9396–9400.
26. Peuchmaur, M., d'Amore, E. S., Joshi, V. V., Hata, J., Roald, B., Dehner, L. P., Gerbing, R. B., Stram, D. O., Lukens, J. N., Matthay, K. K. & Shimada, H. (2003) *Cancer* **98,** 2274–2281.
27. Xu, L. & Massague, J. (2004) *Nat. Rev. Mol. Cell Biol.* **5,** 209–219.
28. Dong, C., Li, Z., Alvarez, R., Jr., Feng, X. H. & Goldschmidt-Clermont, P. J. (2000) *Mol. Cell* **5,** 27–34.
29. Huang, H., Paliouras, M., Rambaldi, I., Lasko, P. & Featherstone, M. (2003) *Mol. Cell. Biol.* **23,** 3636–3645.
30. Krause, A., Zacharias, W., Camarata, T., Linkhart, B., Law, E., Lischke, A., Miljan, E. & Simon, H. G. (2004) *Dev. Biol.* **273,** 106–120.
31. Malki, S., Berta, P., Poulat, F. & Boizet-Bonhoure, B. (2005) *Exp. Cell Res.* **309,** 468–475.
32. Sisson, J. C., Ho, K. S., Suyama, K. & Scott, M. P. (1997) *Cell* **90,** 235–245.
33. Ziegelbauer, J., Shan, B., Yager, D., Larabell, C., Hoffmann, B. & Tjian, R. (2001) *Mol. Cell* **8,** 339–349.
34. Perk, J., Iavarone, A. & Benezra, R. (2005) *Nat. Rev. Cancer* **5,** 603–614.
35. Gill, G. N. (1995) *Structure* **3,** 1285–1289.
36. Kong, Y., Flick, M. J., Kudla, A. J. & Konieczny, S. F. (1997) *Mol. Cell. Biol.* **17,** 4750–4760.
37. Visvader, J. E., Mao, X., Fujiwara, Y., Hahm, K. & Orkin, S. H. (1997) *Proc. Natl. Acad. Sci. USA* **94,** 13707–13712.
38. Niederlander, N., Fayein, N. A., Auffray, C. & Pomies, P. (2004) *Biochem. Biophys. Res. Commun.* **325,** 1304–1311.
39. Higuchi, O., Baeg, G. H., Akiyama, T. & Mizuno, K. (1996) *FEBS Lett.* **396,** 81–86.
40. Loughran, G., Healy, N. C., Kiely, P. A., Huigsloot, M., Kedersha, N. L. & O'Connor, R. (2005) *Mol. Biol. Cell* **16,** 1811–1822.
41. Tobias, E. S., Hurlstone, A. F., MacKenzie, E., McFarlane, R. & Black, D. M. (2001) *Oncogene* **20,** 2844–2853.
42. Iavarone, A., Garg, P., Lasorella, A., Hsu, J. & Israel, M. A. (1994) *Genes Dev.* **8,** 1270–1284.
43. Lasorella, A., Iavarone, A. & Israel, M. A. (1996) *Mol. Cell. Biol.* **16,** 2570–2578.
44. Iavarone, A., King, E. R., Dai, X. M., Leone, G., Stanley, E. R. & Lasorella, A. (2004) *Nature* **432,** 1040–1045.
45. Chenn, A. & Walsh, C. A. (2002) *Science* **297,** 365–369.
46. Yaworsky, P. J. & Kappen, C. (1999) *Dev. Biol.* **205,** 309–321.